# Gata4 is required for maintenance of postnatal cardiac function and protection from pressure overload-induced heart failure

Egbert Bisping*†, Sadakatsu Ikeda*, Sek Won Kong*, Oleg Tarnavski‡§, Natalya Bodyak‡, Julie R. McMullen‡, Satish Rajagopal*, Jennifer K. Son*, Qing Ma*, Zhangli Springer*, Peter M. Kang‡, Seigo Izumo‡§, and William T. Pu*¶

*Department of Cardiology, Children's Hospital Boston, 300 Longwood Avenue, Boston, MA 02115; and ‡Cardiovascular Disease Division, Beth Israel Deaconess Medical Center, 330 Brookline Avenue, Boston, MA 02215

Edited by Eric N. Olson, University of Texas Southwestern Medical Center, Dallas, TX, and approved August 9, 2006 (received for review March 30, 2006)

**An important event in the pathogenesis of heart failure is the development of pathological cardiac hypertrophy. In cultured cardiomyocytes, the transcription factor *Gata4* is required for agonist-induced hypertrophy. We hypothesized that, in the intact organism, *Gata4* is an important regulator of postnatal heart function and of the hypertrophic response of the heart to pathological stress. To test this hypothesis, we studied mice heterozygous for deletion of the second exon of *Gata4* (*G4D*). At baseline, *G4D* mice had mild systolic and diastolic dysfunction associated with reduced heart weight and decreased cardiomyocyte number. After transverse aortic constriction (TAC), *G4D* mice developed overt heart failure and eccentric cardiac hypertrophy, associated with significantly increased fibrosis and cardiomyocyte apoptosis. Inhibition of apoptosis by overexpression of the insulin-like growth factor 1 receptor prevented TAC-induced heart failure in G4D mice. Unlike WT-TAC controls, *G4D*-TAC cardiomyocytes hypertrophied by increasing in length more than width. Gene expression profiling revealed up-regulation of genes associated with apoptosis and fibrosis, including members of the TGF-β pathway. Our data demonstrate that *Gata4* is essential for cardiac function in the postnatal heart. After pressure overload, *Gata4* regulates the pattern of cardiomyocyte hypertrophy and protects the heart from load-induced failure.**

apoptosis | hypertrophy | fibrosis | gene expression | Igf-1

Heart failure is one of the leading causes of morbidity and mortality in industrialized countries (1). An important event in the pathogenesis of heart failure is the development of pathological cardiac hypertrophy (2). This is characterized by increased cardiomyocyte size, increased protein synthesis, and altered gene expression. Over time, the changes in gene expression can be maladaptive and contribute to progression of heart failure (3).

A large body of evidence suggests that the transcription factor *Gata4* is an important regulator of cardiomyocyte hypertrophy (4, 5). *Gata4* has been implicated in the regulation of an array of cardiac genes in response to hypertrophic agonists, including *atrial natriuretic factor* (*ANF*), *brain natriuretic peptide* (*BNP*), *skeletal α-actin*, *α-myosin heavy chain* (*α-MHC*), and *β-myosin heavy chain* (*β-MHC*) (4, 5). *Gata4* overexpression is sufficient to induce the hypertrophic response in cultured neonatal cardiomyocytes and transgenic mice (6). Moreover, the hypertrophic response of cultured neonatal rat cardiomyocytes requires *Gata4* (6, 7).

We sought to investigate the *in vivo* role of *Gata4* in regulating postnatal heart function and the response to hypertrophic stress. Traditional loss-of-function approaches have been complicated by early embryonic lethality in *Gata4* null embryos (8, 9). In our hands, embryos with embryonic cardiac-restricted *Gata4* inactivation also suffered from fetal demise (10). These embryos died from heart failure, and the mutant hearts were characterized by marked myocardial hypoplasia due to decreased cardiomyocyte proliferation (10).

We reasoned that if *Gata4* was a crucial regulator of pathways necessary for cardiac hypertrophy, then modest reductions of *Gata4* activity should result in an observable cardiac phenotype. To test this hypothesis, we used gene-targeted mice that express reduced levels of *Gata4*. We characterized these mice at baseline and after pressure overload. We found that partial *Gata4* deficiency resulted in mild systolic and diastolic dysfunction at baseline and overt heart failure after pressure overload. Our results demonstrate that *Gata4* is required for maintenance of postnatal cardiac function and protection from stress-induced heart failure.

## Results

In this study, we used mice on a uniform genetic background that were heterozygous for deletion of the second exon of *Gata4* (*Gata4*$^{WT/\Delta ex2}$, abbreviated *G4D*), including the start codon and the N-terminal 46% of the coding region (11). To confirm reduction in *Gata4* expression, we performed quantitative real-time RT-PCR (qRT-PCR) and Western blotting on ventricular samples and found that *Gata4* mRNA and protein were reduced in *G4D* mice by 52 ± 5% and by 58 ± 4%, respectively, compared with wild-type littermate controls (WT; $P < 0.05$; Fig. 1 *A–C*). By qRT-PCR, expression of the related transcription factor *Gata6* was unaltered in *G4D* mice (data not shown).

**Mild Systolic and Diastolic Dysfunction in Baseline *G4D* Mice.** At 3 months of age, echocardiography showed normal left ventricular (LV) dimensions but mildly decreased fractional shortening (FS) in *G4D* mice (41.3 ± 3.3% in *G4D* vs. 52.7 ± 2.6% in WT, $P < 0.05$; Fig. 1*D* and Table 1, which is published as supporting information on the PNAS web site), consistent with a mild reduction in ventricular systolic function at baseline. At 8–12 months of age, FS remained mildly depressed in *G4D* mice compared with comparably aged WT littermates (42 ± 4% in *G4D* vs. 55 ± 5% in WT; $n = 4$; $P < 0.05$), suggesting that ventricular dysfunction in these mice is not progressive.

Author contributions: E.B., S. Izumo, and W.T.P. designed research; E.B., S. Ikeda, N.B., S.W.K., O.T., S.R., J.K.S., Q.M., and Z.S. performed research; J.R.M. and P.M.K. contributed new reagents/analytic tools; E.B., S. Ikeda, S.W.K., and W.T.P. analyzed data; and E.B. and W.T.P. wrote the paper.

The authors declare no conflict of interest.

This paper was submitted directly (Track II) to the PNAS office.

Abbreviations: qRT-PCR, quantitative real-time RT-PCR; IgfR, insulin-like growth factor 1 receptor; TAC, transverse aortic constriction; LV, left ventricular; FS, fractional shortening; Dob, Dobutamine; HW/BW, heart weight/body weight ratio.

Data deposition: The sequence reported in this paper has been deposited in the Gene Expression Omnibus (GEO) database, www.ncbi.nlm.nih.gov/geo (accession no. GSE5500).

†Present address: Department of Cardiology and Pneumology, Georg August University, Robert Koch Strasse 40, 37075 Göttingen, Germany.

§Present address: Novartis Institute for Biomedical Research, 101 Technology Square, Suite 6655, Cambridge, MA 02139.

¶To whom correspondence should be addressed. E-mail: wpu@enders.tch.harvard.edu.

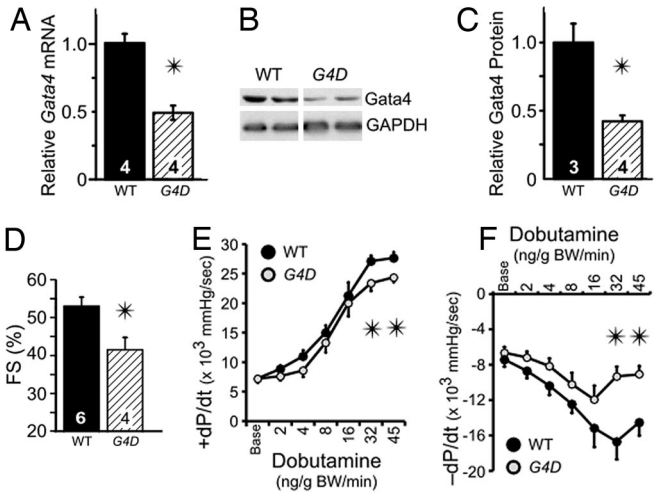


**Fig. 1.** Baseline characterization of *G4D* mice. (*A*) Relative *Gata4* mRNA levels were measured by qRT-PCR and normalized to GAPDH. (*B*) Representative Western blotting for Gata4. (*C*) Relative Gata4 protein levels were measured by Western blotting and normalized to GAPDH. RNA (*A*) and protein (*B* and *C*) were prepared from adult heart ventricles. (*D*) Echocardiography of *G4D* mice showed mildly depressed FS. (*E* and *F*) Measurement of intraventricular pressure during Dob infusion showed decreased contractile reserve and impaired diastolic function in *G4D* mice. In Figs. 1–6, numbers inside bars indicate number of samples per group. For Dob infusion, $n = 6$ per group. *, $P < 0.05$.

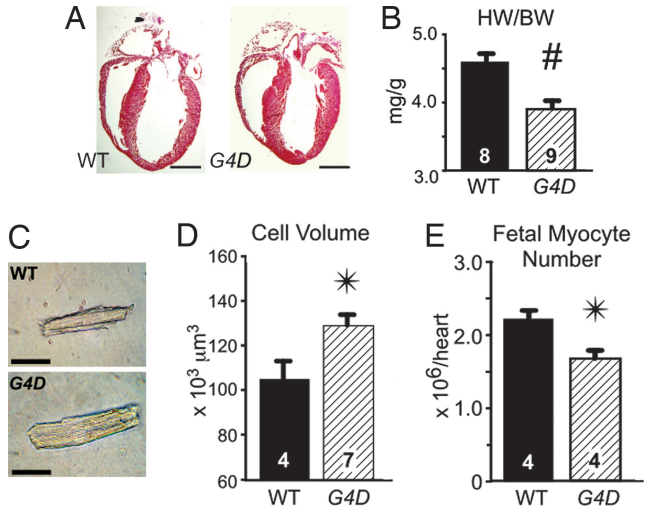


**Fig. 2.** Baseline morphology of *G4D* mice. (*A*) Representative long axis sections through WT and *G4D* adult hearts. *G4D* hearts were structurally normal. (Scale bar, 2 mm.) (*B*) HW/BW ratio was significantly decreased in *G4D* hearts. #, $P = 0.002$. (*C*) Representative dissociated cardiomyocytes from WT and *G4D* hearts. (Scale bar, 50 μm.) (*D*) Volume of *G4D* cardiomyocytes was significantly larger than WT cardiomyocytes. (*E*) Fetal cardiomyocyte number, measured by design-based stereology, was significantly decreased in *G4D* embryonic day 17.5 embryos compared with WT embryos. *, $P < 0.05$.

Invasive hemodynamic measurements with graded i.v. Dobutamine (Dob) infusion revealed that LV pressure and maximal rate of IV pressure rise (+dP/dt) were significantly lower in *G4D* mice at higher Dob doses, indicative of systolic dysfunction and decreased contractile reserve (Fig. 1*E*). In addition, −dP/dt and LV end diastolic pressure (LVEDP), two measures of diastolic function, were abnormal in *G4D* mice. At baseline, LVEDP was significantly higher in *G4D* mice (Table 1). With increasing Dob infusion, *G4D* mice displayed a markedly impaired −dP/dt response (Fig. 1*F*).

**Cardiomyocyte Hypertrophy and Numerical Hypoplasia in Baseline *G4D* Mice.** To determine whether decreased Gata4 expression was associated with altered heart size, we analyzed hearts from 12-wk-old *G4D* and WT mice. *G4D* hearts had normal morphology (Fig. 2*A*), but gravimetric analysis demonstrated a 15% decreased heart weight/body weight ratio (HW/BW) in *G4D* mice (3.9 ± 0.1 vs. 4.6 ± 0.1; $P < 0.01$; Fig. 2*B* and Table 1).

Decreased heart size of *G4D* mice might have been due to a decrease in cardiomyocyte size and/or a decrease in cardiomyocyte number. We measured the size of enzymatically dissociated cardiomyocytes and found that the volume of cardiomyocytes from *G4D* hearts was 22% increased compared with WT controls ($P < 0.05$; Fig. 2*D* and Table 1).

The combination of increased cardiomyocyte size and decreased HW in *G4D* mice suggested that *G4D* mice had decreased cardiomyocyte number. By dividing the relative difference in HW/BW (*G4D*/WT = 0.85) by the relative difference in cardiomyocyte size (*G4D*/WT = 1.22), we calculated that the cardiomyocyte number in *G4D* mice was 70% of wild-type, i.e., a 30% reduction. We previously showed that the level of *Gata4* expression is an important regulator of cardiomyocyte proliferation in the prenatal heart (10). Therefore, we suspected that the decrease in cell number reflected a prenatal decrease in cardiomyocyte proliferation. To test this, we directly measured cell number by design-based stereology in late-gestation embryos (embryonic day 17.5). The measured decrease in cardiomyocyte number (24%; $P < 0.05$; Fig. 2*E*) is consistent with the decreased cardiomyocyte number that we calculated from analysis of adult hearts.

**Overt Heart Failure and Eccentric Hypertrophy After Aortic Constriction.** To determine whether reduction of *Gata4* expression within a physiologically relevant range alters the cardiac response to pressure overload, we performed transverse aortic constriction (TAC; ref. 12). Surprisingly, there was no difference in HW response to pressure overload in *G4D* compared with WT mice, suggesting that hypertrophy on an organ level is not diminished by reduced *Gata4* expression (Fig. 3*A* and Table 2, which is published as supporting information on the PNAS web site). This was not due to normalization of *Gata4* expression after banding, because *Gata4* continued to be expressed at reduced levels in *G4D*-TAC mice (41 ± 7% compared with WT-TAC; $P < 0.05$).

Although there was no difference in the magnitude of hypertrophy between WT-TAC and *G4D*-TAC, the functional response was dramatically different between these groups. WT mice compensated to the pressure load of TAC without change in LV function, LV diameter, or lung weight (Fig. 3 *B* and *C*; Table 2). In contrast, *G4D* mice developed severe LV dysfunction, as measured by FS and LV end diastolic diameter (LVEDD). In the mutant mice, systolic function was severely depressed, with FS decreased to 32.7 ± 2.5%, compared with 50.8 ± 2.6% in banded WT ($P < 0.05$; Fig. 3*B* and Table 2). In addition, the LV of *G4D* mice became dilated, with LVEDD of 3.8 ± 0.1 mm, compared with 3.3 ± 0.1 mm in banded WT ($P < 0.05$; Table 2). This LV dysfunction was associated with pulmonary edema, with lung weight in banded *G4D* mice increasing to 168 ± 12 mg compared with 139 ± 4 mg in banded WT ($P < 0.05$; Fig. 3*C* and Table 2). Thus, pressure overload induced decompensated heart failure in *G4D* mice.

When we analyzed the size and morphology of cardiomyocytes in dissociated cardiomyocyte preparations, we found that *G4D* cardiomyocytes hypertrophied in response to pressure overload to the same degree as WT (Fig. 3*E*). However, the nature of the cardiomyocyte hypertrophic response was different in mutant mice. In WT mice, cardiomyocytes increased in both length and width, so that the ratio of these parameters (L/W) was unchanged. In contrast, hypertrophy of *G4D* cardiomyocytes occurred primarily

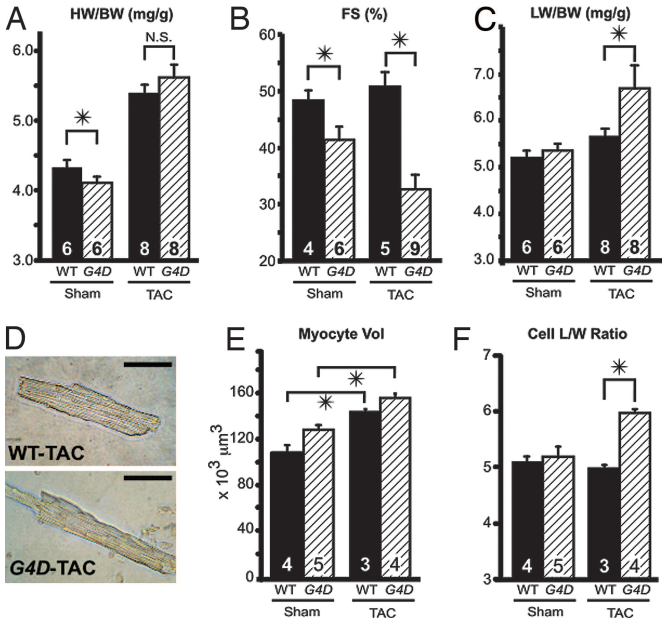


**Fig. 3.** Heart failure and eccentric hypertrophy in *G4D* mice after TAC. (*A*) *G4D* hearts showed the same degree of hypertrophy after TAC as WT heart. (*B*) Systolic function of WT and *G4D* mice after TAC. WT mice compensated for increased afterload and maintained normal FS, whereas *G4D* mice developed severe systolic dysfunction after TAC. (*C*)TAC resulted in increased lung weight in *G4D* mice but did not alter lung weight in WT mice. (*D*) Representative images of dissociated WT and *G4D* cardiomyocytes after TAC. (Scale bar, 50 μm.) (*E*) *G4D* and WT cardiomyocytes increased in size after TAC. (*F*) In WT cardiomyocytes, length (L) and width (W) both increased, so that the length/weight ratio (L/W) was unchanged. In *G4D* cardiomyocytes, length increased out of proportion to width, so that L/W was increased. *, $P < 0.05$.

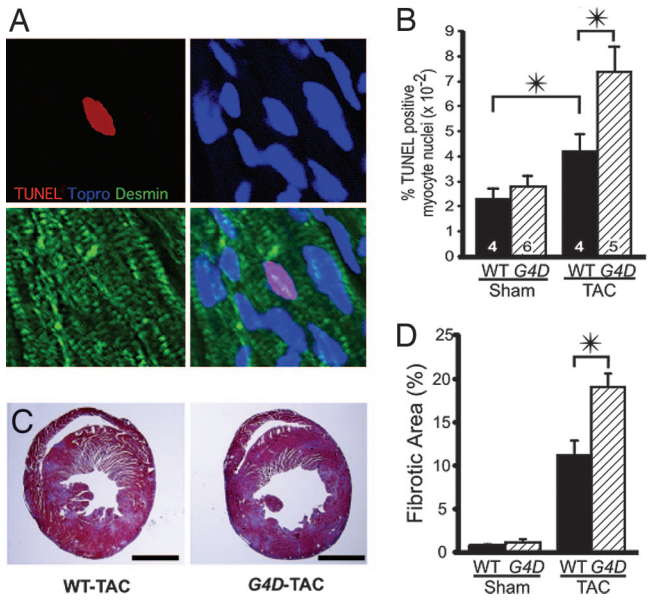


**Fig. 4.** Increased apoptosis and fibrosis in *G4D*-TAC hearts. (*A*) Representative TUNEL staining of *G4D* myocardium. Apoptotic nuclei were labeled by TUNEL (red), counterstained to mark nuclei (Topro-3, blue) and cardiomyocytes (desmin, green), and imaged by confocal microscopy. (*B*) Frequency of TUNEL-positive cardiomyocyte nuclei was increased by TAC. *G4D*-TAC cardiomyocytes had significantly increased apoptosis compared with WT-TAC. (*C*) Post-TAC cardiac fibrosis, demonstrated by Masson's trichrome stain. Concentric hypertrophy of WT-TAC hearts and eccentric hypertrophy of *G4D*-TAC hearts were also evident. (Scale bar, 2.0 mm.) (*D*) The area fraction of fibrotic tissue was increased more in *G4D* hearts compared with WT hearts ($n = 3$). *, $P < 0.05$.

by an increase in cardiomyocyte length, so that the L/W ratio was significantly increased (Fig. 3 *D* and *F*). This pattern typifies eccentric hypertrophy.

**Increased Fibrosis and Apoptosis in *G4D* Mice After TAC.** Because Gata4 deficiency has been associated with increased cardiomyocyte apoptosis (13), we measured the frequency of apoptotic cardiomyocytes by TUNEL staining (Fig. 4*A*). In sham-operated animals, there was no significant difference in the frequency of apoptotic cells between WT and *G4D* genotypes. Pressure overload increased the frequency of apoptotic cardiomyocytes by 1.8-fold in WT mice ($P < 0.05$; Fig. 4*B*). In *G4D* mice, pressure overload resulted in a significantly greater increase in cardiomyocyte apoptosis (3.2-fold; $P < 0.05$ vs. WT-TAC; Fig. 4*B*).

The extent of fibrosis behaved similarly to apoptosis in *G4D* and WT mice. There was no difference between genotypes with Sham operation, but a significantly greater increase in fibrosis in *G4D* compared to WT with TAC operation (19.1 ± 1.6% vs. 11.2 ± 1.7%; $P < 0.05$; Fig. 4 *C* and *D*).

**Unimpaired Hypertrophic Gene Expression in *G4D* Mice After TAC.** To identify genes with altered expression associated with partial Gata4 deficiency, we performed Affymetrix gene expression profiling on ventricular samples from WT and *G4D* mice after sham or TAC operation. Using genotype and operation type in a two-factor ANOVA, we found 792 genes (1,023 probe sets) that were differentially expressed with a $P$ value of <0.001. Among these were genes whose expression is frequently altered in hypertrophy models, including atrial natriuretic factor (*ANF*), brain natriuretic peptide (*BNP*), *skeletal-α-actin* (*Acta1*), β-*MHC*, and *Four and a half LIM domain 1* (*Fhl1*). Although *ANF*, *BNP*, *Acta1*, and β-*MHC* have been reported to be directly activated by *Gata4* (4, 14), partial *Gata4* deficiency did not impair expression of these genes at baseline or after TAC. In fact, β-*MHC* and *Fhl1* were expressed at significantly higher levels in *G4D*-TAC (Fig. 5*A*). To exclude technical issues

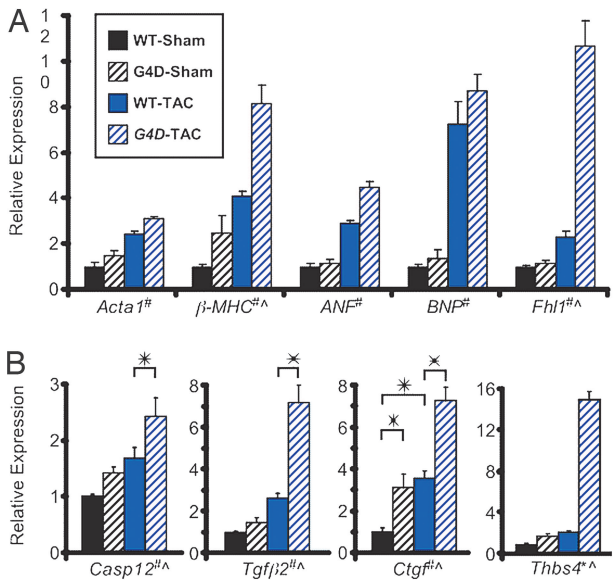


**Fig. 5.** Gene expression analysis. Expression was determined by qRT-PCR (for *BNP*, *Fhl1*, *Casp12*, *Tgfβ2*, and *Ctgf*) or by Affymetrix microarray. (*A*) Relative expression of hypertrophy marker genes. Number of samples per group: WT-Sham, 4; *G4D*-Sham, 4; WT-Band, 6; *G4D*-TAC,6. (*B*) Relative expression of fibrosis and apoptosis associated genes. #, $P < 0.001$ for effect of operation type. ^, $P < 0.001$ for effect of genotype. *, $P < 0.01$ for pairwise comparisons.

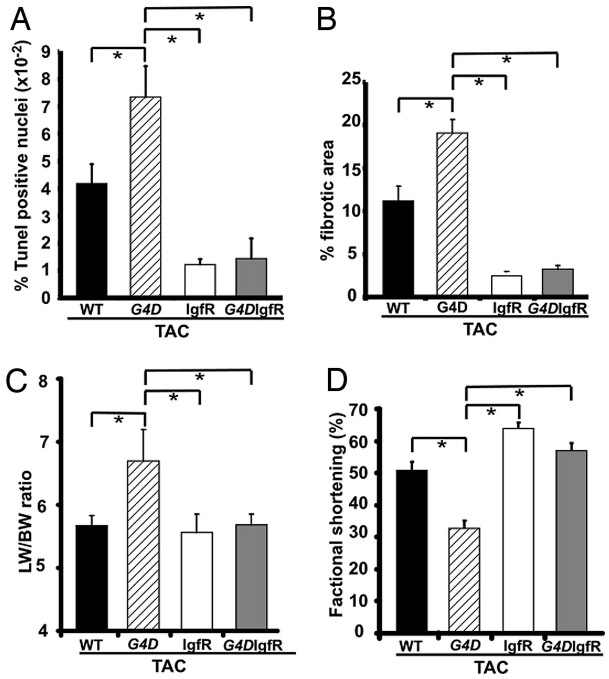


**Fig. 6.** Protective effects of IgfR overexpression. (*A*) TAC-induced increase in frequency of TUNEL-positive cardiomyocyte nuclei was blocked by IgfR and *G4D*-IgfR. (*B*) IgfR and *G4D*-IgfR also blocked the TAC-induced increase in fibrosis. (*C*) TAC-induced increase in the lung weight to BW ratio (LW/BW ratio) in *G4D* was not present in *G4D*-IgfR. (*D*) FS was significantly reduced in *G4D* but not in *G4D*-IgfR. *, $P < 0.05$. IgfR $n = 4$; *G4D*-IgfR $n = 7$.

related to quantitative assessment of gene expression by microarray, we examined the expression of a number of genes independently by qRT-PCR, including *BNP* and *Fhl1*. We found an overall high degree of correlation between the two methods (Table 3, which is published as supporting information on the PNAS web site).

**Profibrotic and Apoptotic Gene Expression in *G4D* Mice.** The pathological phenotype of *G4D*-TAC hearts was characterized by increased fibrosis and apoptosis. ANOVA analysis indicated that 50 genes (54 probe sets) were differentially expressed as a function of the genotype at a *P* value <0.001 (Table 3). Among these genes were several [*Caspase 12*, *Thrombospondin 4*, *Transforming growth factor β2* (*Tgfβ2*), and *Connective tissue growth factor* (*Ctgf*)] that have been reported to be associated with fibrosis and apoptosis and that were markedly up-regulated in *G4D* hearts vs. WT, in particular after application of TAC. We confirmed these results by qRT-PCR (Fig. 5*B*).

**Protection from Apoptosis and Heart Failure by Insulin-Like Growth Factor 1 Receptor (IgfR) Overexpression.** To test the pathophysiological relevance of increased apoptosis in our model, we asked whether suppression of apoptosis would protect *G4D* mice from TAC-induced heart failure. To inhibit apoptosis, we used transgenic mice with cardiomyocyte-restricted overexpression of the IgfR, because increased Igf signaling has well characterized antiapoptotic effects in cardiomyocytes (15–17). IgfR overexpression blocked the increase in apoptosis induced by TAC in both $Gata4^{WT/WT}/IgfR+$ (abbreviated IgfR) and $Gata4^{WT/\Delta ex2}/IgfR+$ mice (abbreviated *G4D*-IgfR; Fig. 6*A*). Accordingly, the extent of fibrosis was significantly lower after TAC in both IgfR and *G4D*-IgfR groups compared with *G4D* (Fig. 6*B*). The reduced apoptosis was associated with protection from TAC-induced heart failure in *G4D*-IgfR mice (Fig. 6 *C* and *D*; $P < 0.05$ vs. *G4D*). This effect was not due to correction of fetal myocardial hypoplasia, because the IgfR transgene did not significantly alter total IgfR expression in the fetal myocardium, and fetal myocyte number was not changed in IgfR transgenics (Fig. 7, which is published as supporting information on the PNAS web site). IgfR overexpression did not alter *Gata4* expression (data not shown).

## Discussion

The development of cardiac hypertrophy is a primary event in the pathogenesis of heart failure (2). In cultured neonatal cardiomyocytes, *Gata4* is an essential mediator of cardiomyocyte hypertrophy in response to mechanical stretch and α-adrenergic stimulation (6, 7). To determine whether variation of *Gata4* activity within a physiologically relevant range influences postnatal function and the response to hypertrophic stimulation *in vivo*, we characterized mice heterozygous for deletion of the second exon of *Gata4* (*G4D*), which express 58% reduced *Gata4* protein (Fig. 1 *A–C*). We found that this degree of *Gata4* deficiency resulted in decreased cardiomyocyte number due to a combination of congenital myocardial hypoplasia (Fig. 2*E*) and increased pressure-overload-induced apoptosis (Fig. 4*B*). Consequently, *G4D* mice had mild systolic and diastolic dysfunction at baseline (Fig. 1 *D–F*) and decompensated heart failure and myocardial fibrosis after pressure overload (Figs. 3 and 4). Partial *Gata4* deficiency did not impair cardiomyocyte hypertrophy after pressure overload but altered the pattern of hypertrophy. *G4D*-TAC cardiomyocytes developed an elongated morphology, reflected at the organ level by eccentric cardiac hypertrophy (Fig. 3). Our results demonstrate that *Gata4* is required *in vivo* for maintenance of normal cardiac function and protection from pressure-overload-induced heart failure. Moreover, our data suggest that modest variations in Gata4 level or activity can have important consequences on cardiomyocyte number, morphology, and cardiac function.

***Gata4* Regulation of Cardiomyocyte Hypertrophy.** Based on *in vitro* loss-of-function studies (6, 7, 18), we hypothesized that *Gata4* activity is an important regulator of cardiomyocyte hypertrophy. Thus, we expected that the reduction of *Gata4* level in *G4D* hearts would result in attenuated cardiomyocyte hypertrophy. However, we found that the magnitude of cardiomyocyte hypertrophy did not depend upon *Gata4* level within the physiologically relevant range of *Gata4* expression examined. At baseline, the average volume of *G4D* cardiomyocytes was increased by 22% over WT (Fig. 2). This was likely a compensatory response to decreased myocyte number and consequently elevated wall stress in *G4D* hearts. Moreover, pressure loading induced a similar degree of hypertrophy in WT and *G4D* cardiomyocytes (Fig. 3). These data do not exclude the possibility that more complete *Gata4* down-regulation would have attenuated the hypertrophic response (see below).

Although the degree of hypertrophy was not different between *G4D*-TAC and WT-TAC mice, the pattern of hypertrophy was qualitatively different. As expected, WT-TAC mice developed changes at the cardiomyocyte level and the organ level that characterize concentric cardiac hypertrophy (Fig. 3). This pattern of hypertrophy results from addition of sarcomeres in parallel and acts to normalize wall stress. In contrast, *G4D*-TAC mice developed changes at the cardiomyocyte and organ levels that characterize eccentric cardiac hypertrophy (Fig. 3). This pattern of hypertrophy results from addition of sarcomeres in series and increases wall stress. The adoption of an elongated cardiomyocyte morphology in eccentric hypertrophy models precedes the development of cardiac dysfunction (19), suggesting this pattern of cardiomyocyte hypertrophy is not a simple epiphenomenon of heart failure. Rather, eccentric hypertrophy results from the activation of specific signaling pathways, such as the mitogen-activated protein kinase 5 (Erk5) pathway (20). We found that Erk5 activity was increased by pressure overload (Fig. 8, which is published as supporting information on the PNAS web site), in agreement with previously reported pressure overload models (21, 22). However, Erk5 pathway activation

was not different between *G4D* and WT mice (Fig. 8). This suggests that signaling pathways other than Erk5 are responsible for the observed eccentric pattern of hypertrophy in *G4D* hearts.

***Gata4* Regulation of Cardiomyocyte Number.** At baseline, we found that *G4D* mice had decreased HW/BW ratio and cardiomyocyte hypertrophy. Based on these data, we calculated a 30% decrease in the number of cardiomyocytes in the adult heart of *G4D* mice compared with WT mice. By direct measurement, we determined that cardiomyocyte number was reduced to a similar degree (24% reduction) in fetal *G4D* hearts. Reduced *Gata4* dosage in fetal cardiomyocytes resulted in decreased cardiomyocyte proliferation (10, 11). Gata4 also promotes cardiomyocyte differentiation from progenitor cells (23). Thus, myocardial hypoplasia in *G4D* mice might result from impaired recruitment of myocyte from progenitor pools in the heart and/or from decreased fetal cardiomyocyte proliferation.

***Gata4* Regulation of Cardiac Apoptosis and Fibrosis.** Increased cardiac fibrosis is a hallmark of pathological cardiac hypertrophy and heart failure. At baseline, *G4D* hearts did not exhibit increased fibrosis. However, after pressure overload, there was increased fibrosis in *G4D* hearts compared with WT hearts (Fig. 4). Cardiac fibrosis adversely impacts diastolic filling (24). Thus, TAC-induced cardiac fibrosis, superimposed on mild baseline diastolic dysfunction seen in *G4D* hearts, likely contributed to decompensated heart failure with pulmonary edema seen in *G4D*-TAC mice.

Because postnatal cardiomyocytes have largely exited from the cell cycle, small increases in the rate of cardiomyocyte death can lead to heart failure by reducing cardiomyocyte number. *Gata4* acted to promote cardiomyocyte survival in a mouse model of doxorubicin-induced cardiomyopathy (13), suggesting that altered cardiomyocyte survival might be important for the development of systolic dysfunction and heart failure in mice with partial Gata4 deficiency. We did not find a difference in cardiomyocyte apoptosis between sham-operated WT or *G4D* mice, suggesting that partial *Gata4* deficiency did not alter the rate of apoptosis at baseline. Consistent with this, cardiac function in *G4D* mice remained stable for >1 year. However, during pressure overload, partial *Gata4* deficiency resulted in a 2-fold increase in the rate of cardiomyocyte apoptosis (Fig. 4). Increased apoptosis in our model was associated with development of severe systolic dysfunction and heart failure (Fig. 3).

To test the hypothesis that increased apoptosis contributed to heart failure in *G4D*-TAC mice, we asked whether suppression of apoptosis by cardiomyocyte-restricted overexpression of IgfR would prevent heart failure in this model. IgfR signaling is strongly antiapoptotic in cardiomyocytes as well as other model systems (15–17). We found that IgfR overexpression blocked the TAC-induced increase in apoptosis and fibrosis and prevented the development of heart failure in *G4D* mice (Fig. 6). The IgfR transgene did not significantly alter fetal IgfR expression and did not rescue the myocyte hypoplasia observed in *G4D* mice (Fig. 7). Thus, prevention of heart failure in *G4D*-TAC mice by IgfR overexpression supports an important role of apoptosis in the pathogenesis of cardiac dysfunction in this model.

***Gata4* Regulation of Cardiac Gene Expression.** ***Hypertrophy marker genes.*** Given that *Gata4* has been reported to be an important regulator of the transcriptional response to hypertrophic agonists, and that *in vitro* Gata4 directly activates the hypertrophic marker genes *ANF, BNP*, β*-MHC*, and *Acta1* (4, 14), we expected that partial *Gata4* deficiency would reduce the baseline expression of these genes or blunt the induction of these genes by pressure overload. We were surprised to find that decreased *Gata4* level did not impair expression of these genes either at baseline or after TAC (Fig. 5*A*). This does not exclude the possibility that expression of these genes requires *Gata4* but was not sensitive to the degree of reduction of *Gata4* levels examined (see below).

***Apoptosis and fibrosis genes.*** We found that apoptosis and fibrosis were significantly increased in *G4D*-TAC mice. By microarray analysis, we identified highly significant up-regulation of genes associated with apoptosis and fibrosis and confirmed selected genes by qRT-PCR. The proapoptotic gene *Caspase 12* was up-regulated in *G4D*-TAC compared with WT-TAC (Fig. 5*B*). *Caspase 12* is a mediator of the sarcoplasmic reticulum-mediated apoptosis pathway (25). Sarcoplasmic reticulum stress-induced apoptosis was recently demonstrated to contribute to heart failure following pressure overload (26).

Expression of *Tgfβ2* and *Ctgf* were highly up-regulated in *G4D*-TAC compared with WT-TAC mice (Fig. 5*B*). TGF-β is a secreted factor that promotes cardiac fibrosis and cardiomyocyte apoptosis (27), and TGF-β activity is increased in human heart failure (27). *Connective tissue growth factor* (*Ctgf*) encodes a secreted polypeptide that acts downstream of TGF-β to induce apoptosis and fibrosis (28). In *G4D*-TAC hearts, *TGF-β2* and *Ctgf* were up-regulated by 2.8- and 2-fold, respectively, compared with WT-TAC hearts, suggesting that activation of the TGF-β signaling pathway contributes to increased apoptosis and fibrosis in *G4D* hearts after pressure overload.

Expression of *thrombospondin-4* (*Thbs4*) was also significantly up-regulated in *G4D*-TAC hearts. *Thbs4* belongs to the thrombospondin family of extracellular glycoproteins, regulating cell adhesion and extracellular matrix generation. It is up-regulated in heart failure models (29, 30). A major role of thrombospondin-1 *in vivo* is to activate TGF-β (31), suggesting that thrombospondin-4 up-regulation might contribute to up-regulation of TGF-β signaling in *G4D*-TAC hearts.

**Importance of Gata4 Gene Dosage in Cardiomyocyte Survival and Hypertrophy.** While this paper was in preparation, Oka *et al.* (32) reported the postnatal phenotype of mice in which Cre/loxP technology was used to ablate *Gata4* in cardiomyocytes (32). A major difference between the *G4D* model and the myocardial knockout models of Oka *et al.* (32) is the degree of perturbation of *Gata4* expression (at the single myocyte level, ≈50% Gata4 reduction in *G4D* vs. complete inactivation in the Oka myocardial knockouts). Thus, the combined data from the two studies represent a *Gata4* allelic series that inform us about the importance of *Gata4* gene dosage in cardiomyocyte survival and hypertrophy. When examined with this point in mind, the convergent and divergent findings in the two studies, summarized in Table 4, which is published as supporting information on the PNAS web site, suggest that *Gata4* is permissive but not dose-limiting for some processes and permissive and dose-limiting for others. In human heart failure, *Gata4* mRNA and protein levels vary by ≈2-fold between normal and failing human hearts (33, 34). Thus, processes in which *Gata4* is dose-limiting within the range interrogated by the *G4D* model are those most likely to be altered downstream of *Gata4* in human heart failure.

The myocardial knockouts reported by Oka *et al.* (32) were characterized by progressive baseline dysfunction associated with increased apoptosis. In response to pressure overload, apoptosis was further increased in the myocardial *Gata4* knockouts (32). Thus, the results of both studies suggest that *Gata4* is required for, and a dosage-limiting regulator of, cardiomyocyte survival, particularly in the face of myocardial stress. Increased baseline apoptosis and progressive deterioration of ventricular function in the myocardial knockout models likely represent a stronger phenotype associated with a greater degree of *Gata4* down-regulation in the myocardial knockout models.

The myocardial knockout and *G4D* models yielded divergent results with respect to cardiomyocyte hypertrophy. Oka *et al.* (32) found that the magnitude of hypertrophy after TAC was significantly blunted in myocardial knockout mice, whereas in *G4D* mice,

it was not affected. This difference suggests that *Gata4* is necessary for cardiomyocyte hypertrophy but is not a dosage-sensitive regulator of this process within the 2-fold range interrogated by the *G4D* model. However, the pattern of hypertrophy is sensitive to a 2-fold change in *Gata4* level, because pressure overload in *G4D* mice resulted in an eccentric rather than concentric pattern of cardiomyocyte hypertrophy (Fig. 3). The pattern of cardiomyocyte hypertrophy in the myocardial knockout models reported by Oka *et al.* (32) was not directly measured, although chamber dilatation with attenuation of LV wall thickening after pressure overload is suggestive of an eccentric pattern.

Inspection of gene expression data from the two studies similarly reveals genes where *Gata4* level may be dose-limiting and those where *Gata4* may be required but not dose-limiting. *Caspase 12* was differentially expressed in both *G4D* and myocardial knockout models (32), suggesting this gene may be an important downstream target of *Gata4*. In contrast, expression of *ANF* and *MHCα* were down-regulated in myocardial knockout models (32), whereas expression of these genes was not affected in the *G4D* model. This difference suggests that whereas expression of *ANF* and *MHCα* require *Gata4*, it is not sensitive to a 2-fold reduction of *Gata4* level. Partial functional redundancy with *Gata6* may have contributed to this result.

## Conclusion

*Gata4* is required to maintain normal myocardial function and to protect the heart from stress-induced heart failure. Reduction of *Gata4* expression within a range relevant for human heart failure results in mild baseline systolic and diastolic dysfunction and sensitizes the myocardium to heart failure after imposition of a pressure overload. Reduction of cardiomyocyte number due to congenital cardiomyocyte hypoplasia and load-induced increased cardiomyocyte apoptosis contribute to the abnormal phenotype. Collectively, our data suggest that pathways that modulate Gata4 level or activity might be important in the pathogenesis of heart failure.

## Materials and Methods

**Mice.** The $Gata4^{\Delta ex2}$ allele was described previously (11). The mice used were all male and on a uniform $F_1$ C57Bl6/J–FVB/N genetic background. On this genetic background, there was no evidence of structural heart disease. $Gata4^{WT/WT}$ littermates from these crosses were used as controls. Transgenic MHCα-IgfR mice, maintained on an FVB/N background, have been described (35). Surgical procedures, physiological measurements, and gravimetric measurements were performed blinded to genotype. TAC was performed by using a modification of our previously described protocol (12). Mice were evaluated 7 days after TAC. Echocardiography was performed by using avertin anesthesia as described (35). Invasive hemodynamics were performed by using a Millar catheter (Millar Instruments, Houston, TX) inserted through the right carotid artery. Dob was infused through a catheter in the left external jugular vein.

**Morphological and Histological Analysis.** Cardiomyocyte dissociation was performed by retrograde collagenase perfusion as described (36). Cardiomyocyte number was measured in embryonic day 17.5 hearts by using a systematic random sampling protocol. Fibrotic area was measured on Masson's trichrome-stained sections as described (35). Apoptotic cardiomyocytes were detected by using the TMR Red *In Situ* Death Detection Kit (Roche, Indianapolis, IN), with myocytes counterstained by Desmin antibody (Biomeda, Foster City, CA).

**Gene Expression.** RNA from ventricles was analyzed on Affymetrix (Santa Clara, CA) 430 2.0 arrays as described (37). Individual gene expression was measured by qRT-PCR by using oligonucleotide sequences listed in Table 5, which is published as supporting information on the PNAS web site.

***Supporting Text.*** Detailed methods are presented in *Supporting Text*, which is published as supporting information on the PNAS web site.

We thank Maria Rivera and Shufen Meng for excellent technical assistance. W.T.P. was supported by the National Heart, Lung, and Blood Institute (Grant P01 HL074734) and by a charitable donation from Edward P. Marram and Karen K. Carpenter. E.B. was funded by a Lilly Fellowship Grant from the German Society of Cardiology.

1. Towbin JA, Bowles NE (2002) *Nature* 415:227–233.
2. Katz AM (1995) *Eur Heart J* 16 Suppl O:110–114.
3. Izumo S, Pu WT (2004) in *Heart Failure: A Companion to Braunwald's Heart Disease*, ed Mann DL (Saunders, Philadelphia), pp 10–40.
4. Pikkarainen S, Tokola H, Kerkela R, Ruskoaho H (2004) *Cardiovasc Res* 63:196–207.
5. Molkentin JD (2000) *J Biol Chem* 275:38949–38952.
6. Liang Q, De Windt LJ, Witt SA, Kimball TR, Markham BE, Molkentin JD (2001) *J Biol Chem* 276:30245–30253.
7. Pikkarainen S, Tokola H, Majalahti-Palviainen T, Kerkela R, Hautala N, Bhalla SS, Charron F, Nemer M, Vuolteenaho O, Ruskoaho H (2003) *J Biol Chem* 278:23807–23816.
8. Kuo CT, Morrisey EE, Anandappa R, Sigrist K, Lu MM, Parmacek MS, Soudais C, Leiden JM (1997) *Genes Dev* 11:1048–1060.
9. Molkentin JD, Lin Q, Duncan SA, Olson EN (1997) *Genes Dev* 11:1061–1072.
10. Zeisberg EM, Ma Q, Juraszek AL, Moses K, Schwartz RJ, Izumo S, Pu WT (2005) *J Clin Invest* 115:1522–1531.
11. Pu WT, Ishiwata T, Juraszek AL, Ma Q, Izumo S (2004) *Dev Biol* 275:235–244.
12. Tarnavski O, McMullen JR, Schinke M, Nie Q, Kong S, Izumo S (2004) *Physiol Genomics* 16:349–360.
13. Aries A, Paradis P, Lefebvre C, Schwartz RJ, Nemer M (2004) *Proc Natl Acad Sci USA* 101:6975–6980
14. Belaguli NS, Sepulveda JL, Nigam V, Charron F, Nemer M, Schwartz RJ (2000) *Mol Cell Biol* 20:7550–7558.
15. Li Q, Li B, Wang X, Leri A, Jana KP, Liu Y, Kajstura J, Baserga R, Anversa P (1997) *J Clin Invest* 100:1991–1999.
16. Li B, Setoguchi M, Wang X, Andreoli AM, Leri A, Malhotra A, Kajstura J, Anversa P (1999) *Circ Res* 84:1007–1019.
17. Butt AJ, Firth SM, Baxter RC (1999) *Immunol Cell Biol* 77:256–262.
18. Liang Q, Wiese RJ, Bueno OF, Dai YS, Markham BE, Molkentin JD (2001) *Mol Cell Biol* 21:7460–7469.
19. Onodera T, Tamura T, Said S, McCune SA, Gerdes AM (1998) *Hypertension* 32:753–757.
20. Nicol RL, Frey N, Pearson G, Cobb M, Richardson J, Olson EN (2001) *EMBO J* 20:2757–2767.
21. Kacimi R, Gerdes AM (2003) *Hypertension* 41:968–977.
22. Takeishi Y, Huang Q, Abe J, Glassman M, Che W, Lee JD, Kawakatsu H, Lawrence EG, Hoit BD, Berk BC, *et al.* (2001) *J Mol Cell Cardiol* 33:1637–1648.
23. Grepin C, Nemer G, Nemer M (1997) *Development (Cambridge, UK)* 124:2387–2395.
24. Kass DA, Bronzwaer JG, Paulus WJ (2004) *Circ Res* 94:1533–1542.
25. Szegezdi E, Fitzgerald U, Samali A (2003) *Ann NY Acad Sci* 1010:186–194.
26. Okada K, Minamino T, Tsukamoto Y, Liao Y, Tsukamoto O, Takashima S, Hirata A, Fujita M, Nagamachi Y, Nakatani T, *et al.* (2004) *Circulation* 110:705–712.
27. Schneiders D, Heger J, Best P, Michael Piper H, Taimor G (2005) *Cardiovasc Res* 67:87–96.
28. Matsui Y, Sadoshima J (2004) *J Mol Cell Cardiol* 37:477–481.
29. Tan FL, Moravec CS, Li J, Apperson-Hansen C, McCarthy PM, Young JB, Bond M (2002) *Proc Natl Acad Sci USA* 99:11387–11392.
30. Rysa J, Leskinen H, Ilves M, Ruskoaho H (2005) *Hypertension* 45:927–933.
31. Crawford SE, Stellmach V, Murphy-Ullrich JE, Ribeiro SM, Lawler J, Hynes RO, Boivin GP, Bouck N (1998) *Cell* 93:1159–1170.
32. Oka T, Maillet M, Watt AJ, Schwartz RJ, Aronow BJ, Duncan SA, Molkentin JD (2006) *Circ Res* 98:837–845.
33. Diedrichs H, Chi M, Boelck B, Mehlhorn U, Schwinger RH (2004) *Eur J Heart Fail* 6:3–9.
34. Hall JL, Grindle S, Han X, Fermin D, Park S, Chen Y, Bache RJ, Mariash A, Guan Z, Ormaza S, *et al.* (2004) *Physiol Genomics* 17:283–291.
35. McMullen JR, Shioi T, Huang WY, Zhang L, Tarnavski O, Bisping E, Schinke M, Kong S, Sherwood MC, Brown J, *et al.* (2004) *J Biol Chem* 279:4782–4793.
36. Shioi T, Kang PM, Douglas PS, Hampe J, Yballe CM, Lawitts J, Cantley LC, Izumo S (2000) *EMBO J* 19:2537–2548.
37. Kong SW, Bodyak N, Yue P, Liu Z, Brown J, Izumo S, Kang PM (2005) *Physiol Genomics* 21:34–42.